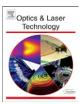
ELSEVIER

Contents lists available at SciVerse ScienceDirect

Optics & Laser Technology

journal homepage: www.elsevier.com/locate/optlastec



Experimental investigation on seam geometry, microstructure evolution and microhardness profile of laser welded martensitic stainless steels

M.M.A. Khan a,*, L. Romoli a, R. Ishak b, M. Fiaschi c, G. Dini a, M. De Sanctis b

- ^a Department of Mechanical, Nuclear and Production Engineering, University of Pisa, Pisa, Italy
- b Department of Chemical Engineering, Industrial Chemistry and Materials Science, University of Pisa, Pisa, Italy
- ^c Continental Automotive Italy S.p.A., Italy

ARTICLE INFO

Article history:
Received 17 July 2011
Received in revised form
10 October 2011
Accepted 12 November 2011
Available online 27 December 2011

Keywords: Laser welding Microstructure Martensitic stainless steel

ABSTRACT

This paper investigates the effects of energy density on geometry of the weld seam and development of microstructures at various weld zones. Energy-based local microhardness profiles are made and linked with the formation of the microstructures. Weld resistance at the interface is energy-limited and seam profile only changes from conical to cylindrical after a certain limit of energy input. Microstructures in the fusion zone changes from cellular to columnar dendritic and equiaxed dendritic with increasing energy input. Variation in morphology of microstructures across the fusion zone is evident within the weld. A distinct region exists in between fusion and heat affected zones due to retention of the primary ferrite. Local microhardness reaches its peak in the fusion zone and decreases gradually from fusion zone to base metal of the outer shell. In the inner shell, peak microhardness occurs in HAZ and the local softening relative to fusion zone and HAZ is visible at the fusion boundary.

© 2011 Elsevier Ltd. All rights reserved.

1. Introduction

Martensitic stainless steels are based on Fe-Cr-C ternary system, undergo an allotropic transformation, and form martensite from austenite under most thermo-mechanical processing situations and air-cooling, which is sufficiently rapid to cause substantial martensite. Normal weld cooling rates are also sufficiently rapid to grow weld metal and HAZ microstructures that are predominantly martensitic as described in [1]. Under normal welding conditions, the austenite present at elevated temperatures will transform to martensite. Many martensite stainless steels retain some high-temperature ferrite in the martensitic matrix, and its existence is a function of the balance of ferrite-promoting to austenite-promoting elements. At higher carbon contents, the austenite phase field expands, promoting fully martensitic structures. A high carbon content results in a harder and more brittle martensite that is more susceptible to hydrogen-induced cracking and possible brittle fracture. Martensitic stainless steels are, therefore, considered being the most difficult of the five stainless steel families to weld as stated in [2]. However, martensitic AISI 416 and AISI 440FSe stainless steels with their chromium and carbon contents are resistant to different environments such as fresh water, steam, crude oil, gasoline, perspiration, and alcohol and also have considerable machinablilty characteristics. Their molybdenum content also provides the elevated-temperature strength through the formation of stable carbide as stated by [1]. Besides, the low-chromium and low-alloy element content make these martensitic stainless steels cheaper than the other types.

Because of their good creep: tensile, and fatigue strength properties in combination with moderate corrosion and heat resistance; and low-cost benefit compared to austenitic stainless steels, both the use and welding of martensitic stainless steels have received considerable interest for engineering application. However, limited investigations have been carried out on weldability and service integrity of such materials. Ping et al. [3] investigated the microstructural evolution of 13Cr-8Ni-2.5Mo-2Al martensitic precipitation-hardened (PH) stainless steel. As the annealing temperature increased, the size and concentration of the precipitates increased concurrently while the number density decreased. The Mo and Cr segregation to the precipitate-matrix interface was detected. The decrease in the strength at higher temperature was due to the formation of larger carbides and reversion of austenite. Berretta et al. [4] studied pulsed Nd:YAG laser welding of AISI 304 and AISI 420 stainless steels in a butt joint configuration. The fillet geometry was not affected by variations in beam position. The weld zone revealed that a fine microstructure was formed, which was dendritic. When the laser beam was shifted in the direction of AISI 420 steel, the structure contained martensite. The HAZ of AISI 420 had the highest microhardness value for any incident laser beam position. Srinivasan [5] examined the effect of the laser beam mode on the microstructural evolution in AISI 410 martensitic stainless steel

^{*} Corresponding author. Tel.: +39 3283693213. E-mail address: muhshin.khan@ing.unipi.it (M.M.A. Khan).

welds. The weld metals consisted of ferrite and martensite in all the welds produced. The hardness variation within the Donut weld metal was much lower than that in the weld metals obtained with the Gaussian mode due to differences in the ferrite fraction. Kurt et al. [2] investigated the effect of austenitic interface layer on microstructure of AISI 420 martensitic stainless steel joined by keyhole plasma transfer arc (PTA) welding process. The weld metal and HAZ were free of cracks. Austenitic interlayer caused to austenite phase and fine needle martensite in the fusion zone. Moreover, austenitic interface laver increased the impact strength of the keyhole welding of the martensitic stainless steel. Raieskhar et al. [6] studied the relative effects of various austenitizing temperatures on microstructure and mechanical properties of electron beam welds of AISI 431 martensitic stainless steel. In the as-welded condition, the microstructure contained dendritic structure with ferrite network and retained austenite in a matrix of un-tempered martensite. Retained austenite content increased with the increase in the austenitizing temperature. Optimum mechanical properties, i.e., strength, hardness, and toughness were observed when austenitized between 1050 °C and 1100 °C followed by tempering. Sharifitabar and Halvaee [7] conducted the resistance upset butt welding of austenitic (AISI 304) to martensitic (AISI 420) stainless steels to explore the effect of welding power on microstructure and mechanical properties of the joint. The results showed that an interlayer composed of 80% ferrite and 20% martensite formed at the joint interface. Different forms of austenite phase and chromium carbide (Cr₂₃C₆) were formed in the HAZ of austenitic stainless steel. The strength and hardness of the joint increased, and HAZ length decreased with the increase in welding power. Gualco et al. [8] investigated the effects of shielding gas, heat input, and post-weld heat treatment on the microstructural evolution of a modified AISI H13 martensitic tool steel. Welding with high heat input resulted in larger carbides precipitation, and a reduction in the retained austenite content and lower hardness.

1.1. Research objectives

As seen from the literatures, fusion zone (FZ) microstructures often contain martensitic dendritic structures with ferrite network, and development of carbides resulting in the highest local microhardness is common in HAZ. Change in weld macrostructures and corresponding mechanical properties under different applied conditions and combination of materials are marked. The size and shape of the weld macrostructure and microstructures seem to be sensitive to variation in materials and joining techniques, joint types, laser beam modes, selected process parameters, and heat input. However, comprehensive examination covering the entire process of laser welding from the definition of the weld bead geometry to the change in microhardness via the development of microstructures and scientific contribution to laser welding making use of energy density, a process variable in the energy term, are rarely available in the literatures. This variable alone enables to provide the same effects as all the selected welding parameters like laser power, welding speed, and spot diameter together do. More work is required for better understanding its influence on the formation of weld bead; the development of weld microstructure; the distribution of principal alloying elements; and hence, the change in local microhardness across the weld. This paper will, therefore, investigate the effects of energy density input on weld seam geometry, microstructure evolution, and change in local microhardness at various weld zones. Experimental studies will be focused on the following:

- effects of energy density input on geometry of the weld seam,
- effects of energy density input on the formation of the weld microstructures at various weld zones, and

 finally, local microhardness profiles at the inner and the outer shells of the overlap joint to show their variations with energy density input, and to relate this change in local microhardness with the formation of microstructures and distribution of ferrite- and austenite-promoting elements.

2. Experimental

The martensitic AISI440FSe and AISI416 stainless steels used in automotive industries for making inner and outer shells of a fuel injector respectively were selected as base materials. Chemical composition of the base metals is reported in Table 2.1. The inside diameter of the outer shell and the outside diameter of inner shell were machined to 7.5 ± 0.025 mm and 7.458 ± 0.015 mm respectively to obtain a clearance between the parts when assembled. The assembled parts were then crimped applying a uniform force of 45 kN around the tip of the outer shell as a replication of the actual fabrication process. In order to remove the dirt from machining, a standard washing procedure stated in EN 1011-6:2005 was followed to clean, cool, and dry the specimens.

Specimens are welded circularly in an overlap joint configuration using a 1.1 kW continuous wave Nd:YAG laser (Rofin DY011). Three controlled parameters are studied in this experiment: laser power (800–1100 W), welding speed (4.5–7.5 m/min), and focus diameter (300–400 μm). The optical system consisted of 300 μm and 400 μm fibers along with two lenses of 200 mm focal length and collimation length are used to deliver the laser with a focal spot diameter of 300 μm and 400 μm , respectively.

Nowadays, energy density is often used in various laser-processing techniques and termed as a key-parameter when continuous-wave laser is used. It correlates the process parameters stated above and expresses them from the energy perspective as described by Berzins et al. [9]. This term is calculated using the same equation as Childs et al. [10] derived

$$ED = \frac{LP}{WS \times \phi_{spot}} \tag{1}$$

Where, ED is energy density; LP is laser power describing the thermal source; WS is welding speed determining the interaction time; and ϕ_{spot} is focal spot diameter defining the area through which energy flows into the material. For the optical system used in this experiment, this focal spot diameter is as same as fiber diameter. According to the Eq. (1), for the aforestated ranges of process parameters, the calculated energy density input is in the range of 19.0–36.9 J/mm².

During the welding operation, the laser beam was focused normally onto the specimen surface. Argon is used as shielding gas with a constant flow rate of 29 l/min to protect weld surface from oxidation, and to suppress the generation of plasma during welding. Experimental conditions for different investigations are given in Table 2.2. After laser welding, no specific heat treatment was carried out. However, inner shell was hardened and tempered prior to welding. Optical micrograph illustrating the weld bead characteristics and SEM micrograph indicating the points

Table 2.1 Chemical composition of the base metals used.

Base metal	Composition (in weight percent)						
	С	Cr	Mn	Si	Mo	S	Se
AISI416 AISI440FSe	0.15 0.60-0.75	13.3 17.2	1.25 1.00	1.00 1.00	0.60 0.75	0.15 -	- 0.20

Download English Version:

https://daneshyari.com/en/article/739574

Download Persian Version:

https://daneshyari.com/article/739574

<u>Daneshyari.com</u>